

ORIGINAL ARTICLE





Concrete fatigue of composite constructions with rib shear connectors

Georgios Christou*,1, Josef Hegger 1, Martin Classen 1,2

Correspondence

Georgios Christou, MSc Email: <u>gchristou@imb.rwth-aachen.de</u>

Affiliations

¹ RWTH Aachen University Institute of Structural Concrete Mies-van-der-Rohe-Straße 1 52074 Aachen, Germany ²KU Leuven Construction Technology, De Nayer (Sint-Katelijne-Waver) Campus Jan Pieter de Nayerlaan 5 2860 Sint-Katelijne-Waver, Belgium

Abstract

Rib shear connectors are gaining increasingly attention in the field of composite constructions. Especially in bridge constructions, rib shear connectors offer many advantages compared to conventional composite shear connectors such as headed studs. In order to describe the load-bearing behaviour of rib shear connectors under cyclic loading, the successively increasing slip resulting from the cyclic loading of the shear connectors must be taken into account. The latter leads to the growth of the relative displacements along the composite joint and thus, to the degradation of the previously rigid shear connection. This effect leads to rearrangements of internal forces between the composite partners through which the load bearing behaviour and load bearing capacity of the structure alter. In this article results of experimental investigations on two cyclic single Push-Out-Tests (sPOT) and one full-scale girder test regarding the degradation of the composite interconnection are presented and analysed. The investigated shear connectors in the full-scale girder test are subjected to a comparable load history to that of the connectors in the sPOT. The results give insight into the effects of the degradation of the shear connection, as previously seen in sPOT, on the overall load bearing behaviour of composite girders.

Keywords

Composite constructions, rib shear connectors, shear connection degradation and fatigue, experimental investigations

1 Introduction

The advantages of composite constructions such as the speed of construction, the performance and the value can be enhanced by the usage of rib shear connectors instead of currently popular alternatives such as headed studs. Especially in the field of bridge construction, where cyclic loading occurs, welded headed studs often constitute the weakest component of composite girders and do not allow the efficient deployment of the two components steel and concrete. Furthermore, the usage of rib shear connectors leads to higher stiffness as well as the higher maximum load-bearing capacity of the composite connection due to which greater span lengths can be achieved.

While the usage of rib shear connectors under static loading has been investigated sufficiently both with experimental and theoretical studies (e.g.: [1][2][3]), current regulations regarding such connectors are very conservative in case of cyclic loading due to the limited available information. Thus, experimental investigations with cyclic loading were conducted to provide information regarding fatigue failure of composite girders with rib shear connectors. The current paper presents results of two cyclic single Push-Out-Tests and one full-scale composite girder, in which the composite connection is achieved by clothoid-shaped rib shear connectors, under cyclic loading.

2 State of the art

Currently available studies include just a few experimental investigations regarding fatigue behaviour of composite constructions with rib shear connectors. Most of the available research results offer hereby incomplete information regarding the fatigue behaviour of these connectors. Experimental investigations conducted in [4] and [5] had to be interrupted before fatigue failure could be achieved due to early failure of the test rig. Thus, it was not possible to investigate the circumstances under which fatigue failure in the interconnection occurs. Rib shear connectors have also been tested under cyclic tensile forces in [6]. Here, a model for calculating the lifespan in case of fatigue failure in the form of concrete pry-out could be derived. Further investigations followed in [7]. Here, a new test rig was deployed which led to promising results regarding fatigue failure of rib shear connectors under cyclic shear loading. Additional investigations and analysis of the results led to an engineering model in [8]. The latter allows the calculation of the lifespan of rib shear connectors in case of cyclic pry-out failure depending on loading parameters and the static dowel characteristic curve of the rib shear connectors. Further investigations regarding rib shear connectors under static and cyclic loading were conducted in [9]. Investigation focusing on the steel fatigue of composite girders are included in [10] and [11]. The former publication included numerical and experimental investigation on rib shear connectors, while the

© 2021 Ernst & Sohn Verlag für Architektur und technische Wissenschaften GmbH & Co. KG.

This is an open access article under the terms of the Creative Commons Attribution-NonCommercial-NoDerivs License, which permits use and distribution in any medium, provided the original work is properly cited, the use is non-commercial and no modifications or adaptations are made.

latter focused on the fatigue behaviour of composite girders with hot-dip galvanized rib shear connectors.

Full-scale composite girders with rib shear connectors were investigated in [5]. Nevertheless, the investigations presented here regard girders with ultra high strength concrete (UHPC) and are therefore not comparable with the herein presented tests.

3 Experimental investigations

3.1 General

In addition to the experimental investigation conducted in the past regarding the load-bearing behaviour of single connectors, representative full-scale tests are needed to evaluate the load-bearing behaviour of the connectors under realistic loading conditions. One main aspect, which is (deliberately) neglected in single Push-Out-Tests and which is expected to influence the characteristics of the composite interconnection, is the statically indeterminate system which occurs due to multiple connectors positioned in each shear field.

Considering a 4-point bending test in which the shear force in each shear field is presumed to be evenly distributed in the available connectors along the axis, the shear force in some of the connectors is underestimated. Nevertheless, ductile connectors, such as the rib shear connectors used here, allow relocation of a percentage of the shear force in other less loaded connectors.

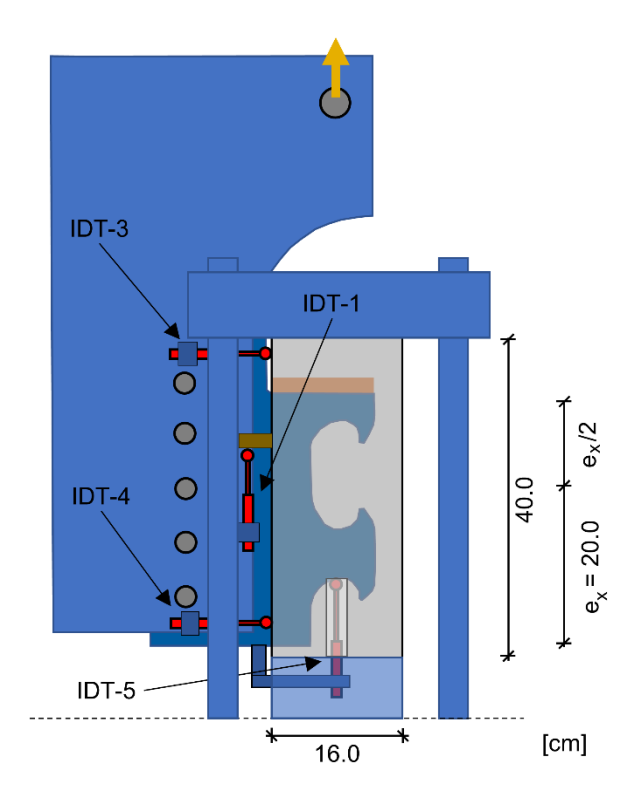


Figure 1: Test setup sPOT

To compare the load-bearing behaviour of the connectors tested in the sPOT with that of the connectors in a full-scale girder, the planned composite girder was and tested in accordance to the test parameters (and results) of the sPOT Dyn_D_6.1 and Dyn_D_6.2 presented in [7]. Both Dyn_D_6.1 and Dyn_D_6.2 were identical and were tested as demonstrated in Figure 1, while the geometry of the tested girder is shown in Figure 2.

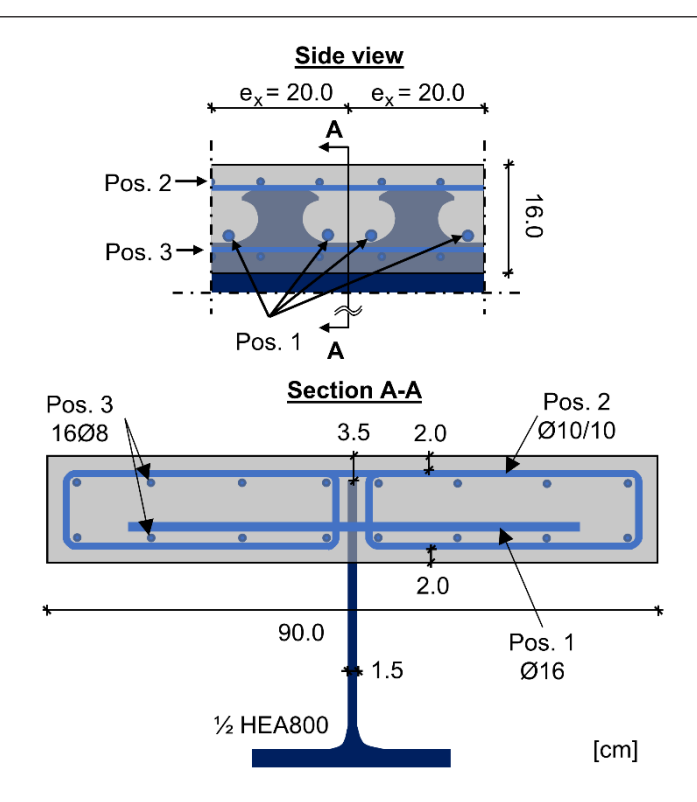


Figure 2: Side view and section of the tested composite girder

3.2 Test parameters

While the concrete slab in the sPOT had a width and length of 40 cm respectively as opposed to the concrete slab of the girder with a width of 90 cm, the geometrical parameters which influenced the load-bearing capacity of the connectors were identical. Thus, the upper embedment depth of the shear connectors was chosen to 35 mm. For the rib shear connectors tested a dowel distance of $e_x = 200$ mm and a clothoid-dowel geometry was chosen as shown in Figure 1 and Figure 2. While the thickness of the steel web in case of the sPOT was chosen to 20 mm, the used steel beam in case of the full-scale girder test (HEA800) consisted of a web with a thickness of 15 mm. For the steel used for the sPOT as well as for the halved HEA800 beams the steel class S355 was chosen. The reinforcement of the concrete belts (B500B) consisted of rebars with a diameter of 8 mm along the axis of the girder, stirrups with a diameter of 10 mm and 2 rebars with Ø16 crossing each concrete dowel as shown in Figure 2. Furthermore, the concrete class was chosen to C30/37 and the thickness of the concrete slab was chosen to 16 cm both for the sPOT and for the composite girder.

The sPOT were loaded with an upper load of 225 kN. The load range was chosen to 75 kN. The girder with a span of 6.6 m was loaded with two single loads. The single loads were positioned at a distance of 3.0 m from the supports. The upper limit and the range of every single load was chosen to 400 kN and 150 kN respectively. In the given static system (Figure 9) the applied loads led to a maximal shear force of 400 kN and a minimum shear force of 250 kN. The corresponding moment equals 1.2 MNm and 0.75 MNm respectively. In case of the chosen composite girder, for which a halved HEA800 steel beam was used, a lever arm z of approximately 38 cm occurred. Depending on the state of the composite interconnection or rather of the slippage, which increased as the number of the applied load cycles grew, the lever arm decreased. Thus, the shear force transmitted in each shear field calculated as followed (equations (1) and (2)) is an approximation.

$$P_{total,max} = \frac{\Delta M}{z} = \frac{1,2-0}{0,38} = 3,16 MN$$
 (1)

$$P_{total,min} = \frac{\Delta M}{z} = \frac{0.75 - 0}{0.38} = 1.97 MN \tag{2}$$

In each of the two shear fields formed between the supports and the single loads, 14 steel dowels were available. Thus, the equivalent load in each Dowel can be calculated as shown in the equations (3) and (4):

$$P_{Dowel,max} = \frac{P_{total,max}}{n} = \frac{3,16}{14} \times 10^3 = 226 \, kN$$
 (3)

$$P_{Dowel,min} = \frac{P_{total,min}}{n} = \frac{1.97}{14} \times 10^3 = 141 \, kN$$
 (4)

While the web thickness does not influence the calculative load-bearing capacity in case of pry-out failure, the thinner web leads to a lower dowel stiffness. Thus, the girder was expected to develop a higher slippage at the end of the planed 2 Mil. load cycles. According to the observations made in [8], cyclic pry-out failure is a slippage-dependent failure mode as opposed to pry-out failure under static loading. Thus, fatigue failure in case of cyclic pry-out can be assumed to be reached faster in the girder test. In [12] a model for calculating the stiffness of the rib shear connectors was introduced. Taking into account the three stiffness components consisting of bending and shear stiffness of the steel dowels as well as the stiffness of the concrete dowels, the overall dowel stiffness C_{VD} can be calculated.

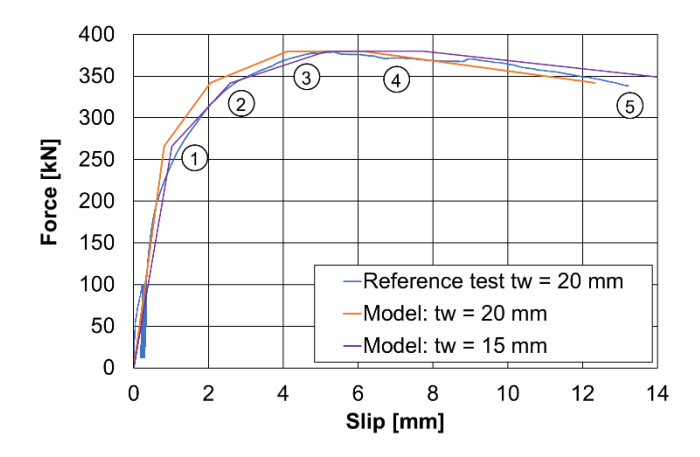


Figure 3: Experimental and calculative characteristic dowel curves

Figure 3 shows the result of a static reference test executed before the sPOT Dyn_D_6.x (t_w = 20 mm), as well as the calculative characteristic dowel curves for a 15 mm- and a 20 mm thick steel web according to [12]. It is apparent, that the web thickness has only a minor influence on the dowel stiffness. The load-bearing capacity of the reference test equalled roughly 375 kN, while the deformation capacity of the dowel amounted to approx. 13 mm.

Taking into consideration the load-bearing capacity of the dowels as found in the static reference test, the relative upper load corresponding to the chosen upper load of 225 kN was equal to λ_u = 0.6, while the relative load range amounted to approx. λ_u = 0.2.

Last but not least, the degree of the shear connection for the given geometric and material parameters of the girder and those of the rib shear connectors reached $\eta\approx 1.0$. The chosen loads lead to (calculative) elastic strains in the girders cross-section with the assumption of a rigid shear connection. A higher shear load in the shear fields could not be achieved without reaching the yield strength of the used materials in the area between the applied single loads.

3.3 Experimental procedure and measurements

Both the sPOT and the girder followed the same test procedure. In

the beginning, the load was applied path-dependent following which 60 slow load cycles took place to record in detail the effects that took place in that period. Hereafter the loading was applied force-controlled with a frequency of approx. 4,9 Hz in the sPOT and 1,2 Hz in the girder test. The latter had to be adjusted (decreased) over the lifespan due to the increasing deflection leading to higher oil consumption. After every 0,1 million load cycles, the sPOT and the girder test got relieved and re-loaded to record the static dowel stiffness and the overall girder stiffness respectively.

In each of the two sPOT, five inductive displacement transmitters (IDT) were applied. Two IDTs were used to record the slip along the steel web axis. The two IDTs were placed mirrored in the left and right side of the steel web. The results of these two IDTs were averaged to eliminate inaccuracies. Two further IDTs (IDT-3 and IDT-4) were deployed in order two record the horizontal displacement of the concrete slab regarding the initial position of the steel web. Through the two measured horizontal displacements in the upper and bottom edge of the specimen, the rotation of the specimen could be derived. One further IDT (IDT-5) was applied behind the load-carrying steel dowel as shown in Figure 1 to record the percentage of the slip which resulted from the bending and shear shift of the steel dowel. This paper concentrates on the measurement of the slip in the composite interconnection.

The measurements of the girder (as shown in Error! Reference source not found. Figure 9) were also concentrated around the slip development in the shear connection. For each shear field, seven IDT were provided and were placed equidistantly along the axis of the girder with a spacing of twice the dowel spacing (40 cm). Furthermore, one IDT was placed in each girder-ending (AA and OO) to record the descending slip in the area of the supports. Last but not least, one IDT was applied to record the deflection of the girder. To capture the force redistribution in the cross-section, resulting from the increasing slip in the composite connection, strain gauges were applied on the steel beam and concrete belt of the composite girder. In axis A, C, E and G a total number of 20 strain gauges were applied as shown in Figure 4.

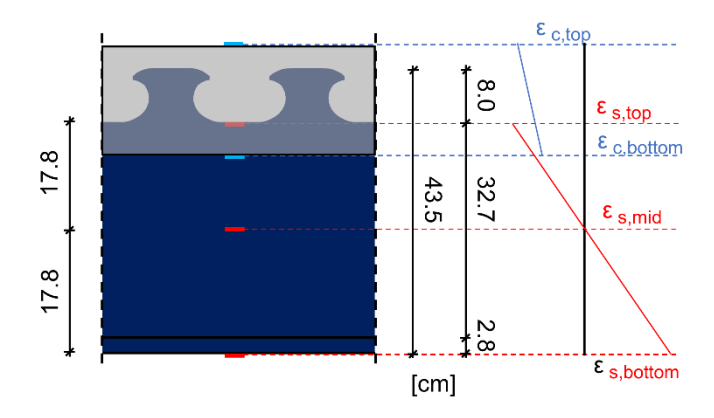


Figure 4: Strain gauges in the cross-sections of the girder

3.4 Test results

3.4.1 Single Push-Out-Tests

Figure 5 shows the slip-load cycle curves of the two single Push-Out-Tests which were recorded through two IDT's for each sPOT (IDT-1 and IDT-2 in Figure 1). The shown curves correspond to the mean slip measured in each test specimen. The minor deviation between the slip of the two dowels is tolerable and both connectors show an overall very similar behaviour. Furthermore, Figure 5 re-

veals the proportion of the overall slip owing to an elastic and an inelastic slip. While the former amounts to only approx. 20% of the overall slip, the inelastic slip is dominant and amounts to approx. 80% of the total slip. Although the load parameters were chosen within the borders of the approximately linear behaviour of the dowels (Figure 3,0 \rightarrow 260 kN) inelastic slip occurs right after the first load cycles. Nevertheless, a strong slip increase is only noticeable within the first $5\cdot10^5$ load cycles, while hereafter the slip remains roughly constant.

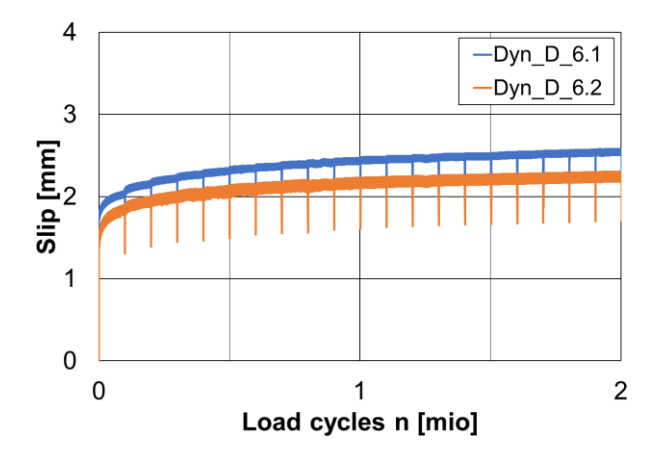


Figure 5: SPOT results - slip-load cycles curve

3.4.2 Girder test

The girder test ran for 26 days to complete 2 million load cycles inclusive static relief and reloading after each 0.1 million load cycles. Figure 6 shows the deflection of the girder in the middle of the beam which represents its overall load-bearing behaviour over its lifespan. The stiffness of the girder decreased within the first $5\cdot 10^5$ load cycles rapidly which is translated into a strong deflection increase within this period. Hereafter a constant jet insignificant decrease of the stiffness took place. The load-bearing behaviour of the girder reflected in the deflection-load cycle curves is in agreement with the increasing slip of the sPOT over their lifespan.

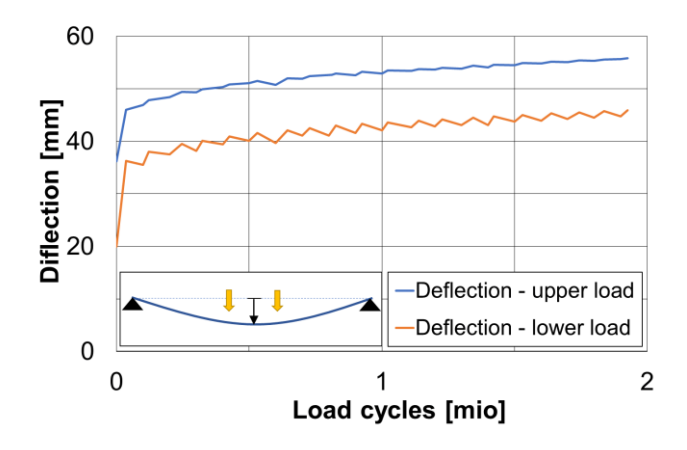


Figure 6: Deflection of the girder by upper and trough load

While the deflection of the girder gives an overview regarding the overall load-bearing behaviour of the girder over its lifespan, the development of the slip along the girder axis gives insights into the load history of the individual dowels. The measurements presented in Figure 7, in which the results of the slip measured in each axis (AA to G and I to OO), confirm the expected non-linear slip- and load distribution in the individual shear connectors. Within the first 10^4 load cycles, the slip in the area of the inner and outer dowels (near axis AA and G, as well as I and OO) increases to approx. $0.5 \, \text{mm}$, while the

slip in the area of the decisive dowels (between axis B and D as well as M and O) reaches approx. 1.0 mm. Taking into consideration the characteristic dowel curve presented in Figure 3 it can be assumed that the load in the outer and inner dowels amounts to approx. 50% in comparison to the shear load in the decisive dowels. In opposite to the simplified assumption for the design, that the shear force is equally distributed to the available dowels within the shear field, Figure 7 reveals the higher exploitation of the dowels in the decisive areas, resulting from the increased slip.

Nevertheless, the ductility, which these shear connectors provide, allows the redistribution of the shear forces in other less exploited dowels, through which the unequal slip over the girder axis can be compensated. After roughly $4\cdot10^5-5\cdot10^5$ load cycles the slip in the inner and outer dowels had reached approx. 1 mm and thus, the resulting shear force in each shear field can be assumed to be distributed roughly equally to the available dowels in the shear field.

Furthermore, as shown in Figure 7, the slip in the area of the girder with the decisive dowels reaches after 2.0 million load cases approx. 2.5 to 2.8 mm which is similar to the maximum slip found in the sPOT. The affected and most loaded dowels are located at a distance of approx. 60-70 cm from the supports which equals approx. 1.5 times the lever arm z.

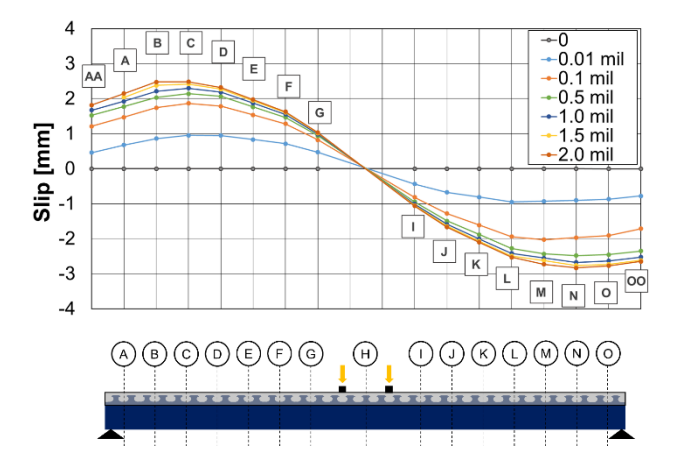


Figure 7: Slip along the girder axis

Figure 8 shows a comparison of the slip development of the dowels in the two sPOT and one decisive dowel of the girder (axis N). While the overall behaviour of the three compared connectors follows the same pattern, it is obvious, that the slip in the area of the decisive shear connector in the composite girder increased faster than the slip of the dowels in the sPOT. This can be traced back to the initially higher loading of this dowel as described above. Taking into consideration that the first $4\cdot10^5\text{-}5\cdot10^5$ load cycles are decisive for the overall slip increase and that within these load cycles the shear force is roughly affine to the slip, the higher slip developed in the shear connector of the girder can be explained.

The strains measured in the cross-sections in axis A, C, E and G are presented in Figure 10. The strains measured over the height of the concrete beam as well as of the steel beam (S) increase linear with increasing distance from the upper concrete edge. The increasing inclination of the linear curves describing the strains over the height of the beam is a result of the growing slip in the shear connection. While the concrete slab is mainly subjected to compression and both the upper and the bottom strain measured decrease with increasing load cycles, the absolute value of the strains measured in the top and in the bottom edge of the steel beam increases leading to higher

compression in the top half and higher tension stresses in the bottom half of the steel girder. While the slip in the area of axis C is higher than in the other areas of the shear field, the strain alteration over the lifespan in this axis is less than in any other axis measured.

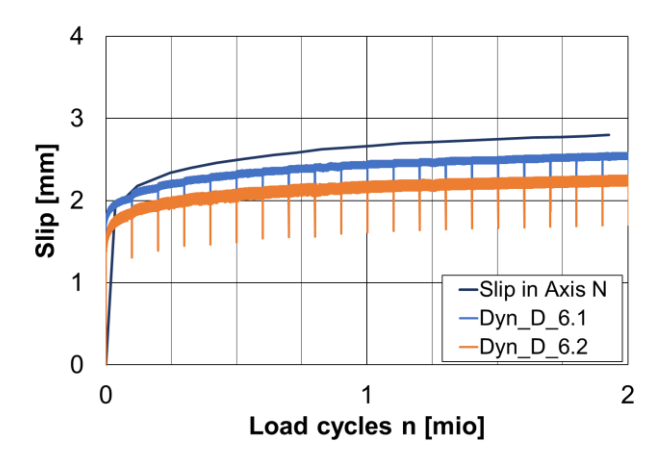


Figure 8: Comparison of sPOT and decisive girder dowel

4 Conclusion

In the present paper, the results of experimental investigations regarding fatigue of rib shear connectors are discussed. The loadbearing behaviour of single Push-Out-Tests under cyclic loading was compared with that of the individual shear connectors of a fullscale girder. The latter was subjected to a loading which resulted to a comparable loading history for each of the bearing shear connectors to that of the sPOT. The slip development over the lifespan of the rib shear connectors, which resulted from the two test variations (sPOT and the girder test), were in agreement. Furthermore, the assumption of a rigid connection and a linear strain distribution over the height of the composite girder, as a result of a shear connection grade of η = 1.0, could not be verified in the investigated girder test. The increasing gap between the strain in the bottom concrete edge and the upper steel edge, resulting from the growing slip in the shear connection, is present in the investigated girder. The degradation of the shear connection mainly takes place within the first 104-5·105 load cycles, while hereafter the properties of the shear connectors change roughly. Overall, the investigated rib shear connectors demonstrated very good load-bearing behaviour under the applied cycling loading. Further investigations in girders with rib shear connectors and shear connection grades below 0.8 are necessary to collect information regarding fatigue failure in the shear connection.

Acknowledgement

This research work has been funded by the German research foundation (DFG) and is part of the research project "Fatigue behaviour of rib shear connectors under consideration of the interacting damage processes of steel and concrete", project number 287311725 (HE 2637/26-1, FE 459/6-1). The researchers would like to express their thanks for the support.

References

- [1] Lorenc, M. et al.: The behaviour of puzzle-shaped rib shear connectors Part I: Experimental study. Journal of Constructional Steel Research 101, pp. 482-499, 2014.
- [2] Kopp, M. et al.: Rib shear connectors as shear connectors for composite beams–Background to the design concept for static loading. Journal of Constructional Steel Research, 147, pp. 488-503, 2018.

- [3] Classen, M.; Hegger, J.: Shear tests on composite dowel rib connectors in cracked concrete. In: ACI Structural Journal, vol. 115, No. 3, pp. 661-671, 2018.
- [4] Classen, M.; Gallwoszus, J.: Concrete fatigue in composite dowels. In: Structural Concrete, vol. 17(1), pp. 63-73, 2016.
- [5] Gallwoszus, J.: Fatigue of composite constructions with composite dowels. Aachen, RWTH Aachen University, Dissertation, 2015.
- [6] Classen, M.; Gallwoszus, J.; & Stark, A.: Anchorage of rib shear connectors in UHPC under fatigue loading. In: Structural Concrete, vol. 17(2), pp. 183-193, (2016).
- [7] Christou, G., Ungermann, J., Wolters, K., Hegger, J. and Claßen, M. (2020): Ermüdung von Verbunddübelleisten experimentelle Untersuchungen. In: Stahlbau. doi:10.1002/stab.201900103
- [8] Christou, G., Ungermann, J., Wolters, K., Hegger, J. and Claßen, M. (2020): Ermüdung von Verbunddübelleisten Analyse und Modellentwicklung. In: Beton- und Stahlbetonbau. doi:10.1002/best.201900091
- [9] Ahn, J. H.; Kim, S. H., Jeong, Y. J.: Shear behaviour of perfobond rib shear connector under static and cyclic loadings. In: Magazine of Concrete Research, Vol. 60, Is. 5, pp. 347-357, 2008.
- [10] Feldmann, M.; Kühne, R.; Ungermann, D.; et al.: Ermüdungsfestigkeit feuerverzinkter Verbunddübelleisten. In: Bauingenieur 94, vol. 6, pp. 206-215, 2019.
- [11] Wolters, K.; Christou, G.; Feldmann, M.: *Untersuchungen* zum Risswachstum in Verbunddübelleisten. In: Bauingenieur 94, vol. 6, pp. 216-227, 2019.
- [12] Classen, M.; Hegger, J.: Shear-slip behaviour and ductility of composite dowel connectors with pry-out failure. In: Engineering Structures, vol. 150, pp. 428-437, 2017.

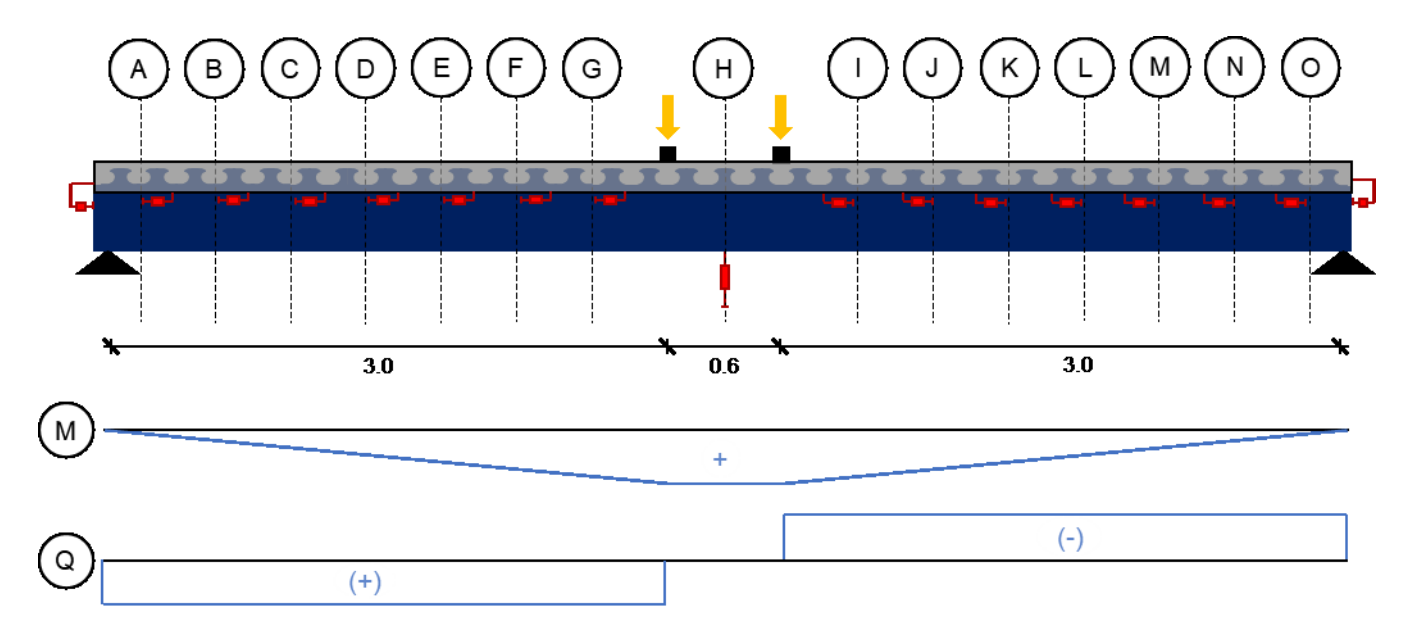


Figure 9: Static system and slip measurement

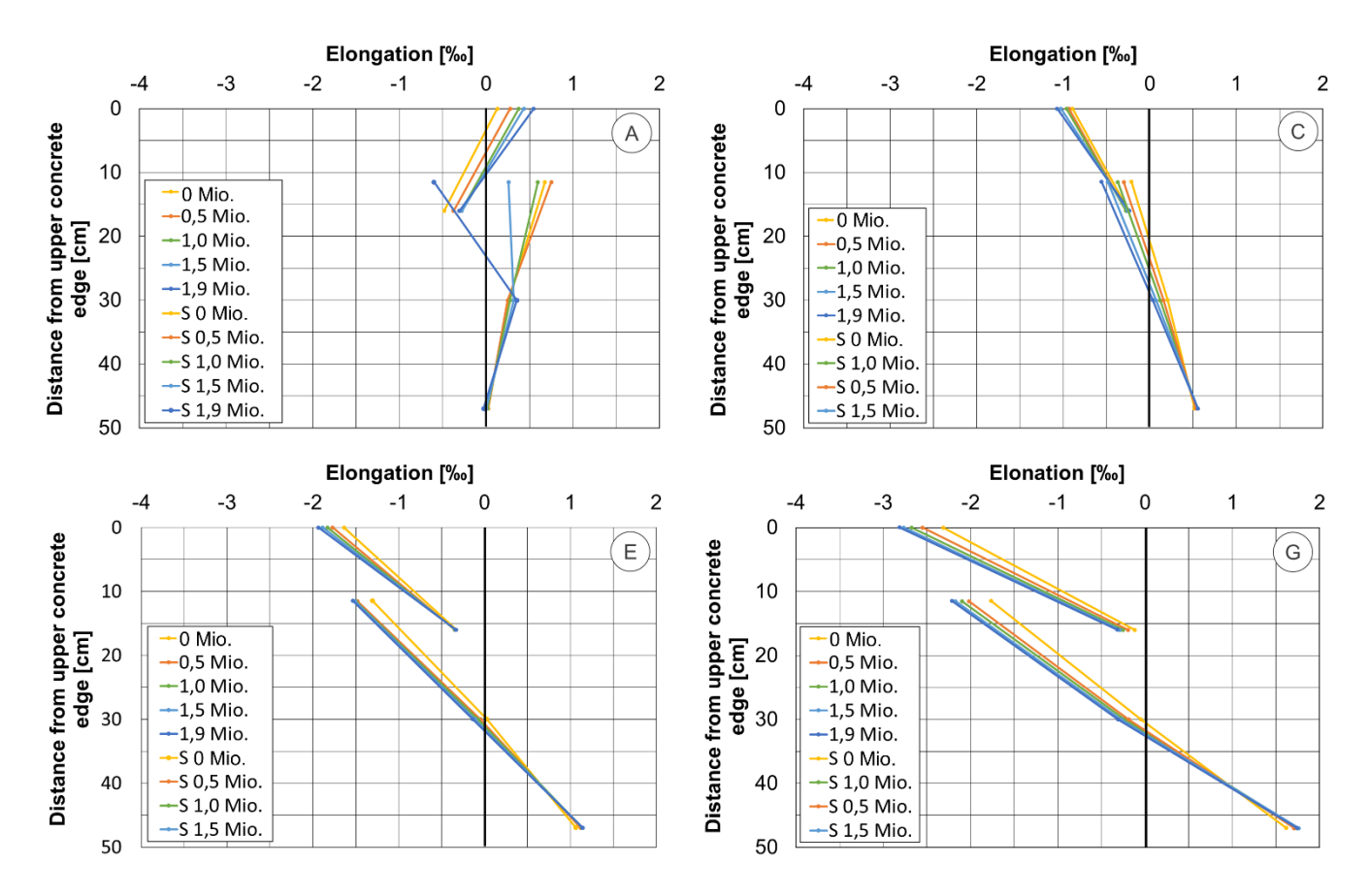


Figure 10: Strains in the cross-sections in axis A, C, E and G